

The Study of Corrosion and Wear Resistance of Copper Composite Coatings with Inclusions of Carbon Nanomaterials in the Copper Metal Matrix

Viktorija MEDELIENĖ^{1*}, Vojtech STANKEVIČ², Asta GRIGUCEVIČIENĖ¹, Aušra SELSKIENĖ¹, Gedvidas BIKULČIUS¹

¹Institute of Chemistry of Center for Physical Sciences and Technology, A. Goštauto 9, LT-01108 Vilnius, Lithuania

²Semiconductor Physics Institute of Center for Physical Sciences and Technology, A. Goštauto 11, LT-01108 Vilnius, Lithuania

Received 27 November 2010; accepted 01 June 2011

This paper deals with the peculiarities of the behaviour of copper nanocomposite coatings with CNMs inclusions under the free corrosion conditions in the acidic medium. The parameters of corrosion current density (j_{corr}), anodic dissolution current density (i_a) and polarization resistance (R_p) have been determined. In the acidic medium a stronger oxidation of nanostructured copper nanocomposites occurred. With longer immersion periods more corrosion products are formed, resulting in a increase in the polarization resistance (R_p) of corrosion. Corrosion products cover the whole surface of the coatings and the corrosion rate (j_{corr}) tends towards a steady value of $1.7 \times 10^{-3} \div 2.1 \times 10^{-3} \text{ A} \cdot \text{cm}^{-2}$ for all copper coatings studied: $1.7 \times 10^{-3} \text{ A} \cdot \text{cm}^{-2}$ for both Cu and Cu-CNM1, $1.9 \times 10^{-3} \text{ A} \cdot \text{cm}^{-2}$ – for Cu-CNM2 and $2.1 \times 10^{-3} \text{ A} \cdot \text{cm}^{-2}$ – for Cu-CNM3 composite coatings. It has been established that nanocomposites possess a higher wear resistance as compared to that of pure copper. The damage of metal characterized as a depth scar (\bar{d}) is lower. The roughness of the composites studied was found to be the essential factor affecting their wear resistance. Therefore, the wear resistance of nanocomposites is impaired when they are deposited on a hard steel substrate.

Keywords: copper, carbon nanoderivatives, nanocomposites, corrosion, wear.

INTRODUCTION

Graphite oxide sheets, now named as graphene oxide, which is the product of chemical exfoliation of graphite have been known for more than a century. Interest in this old material has been resurged after the discovery of graphene, as graphite oxide is considered to be a promising precursor for bulk production of graphene [1–3].

According to the latest fashion in science, chemists view graphene/or graphene oxide as an unconventional type of a soft material and it possesses characteristics of polymers, membranes, colloids and amphiphiles [4, 5]. Graphene has been considered by many physicists as a revolutionary material with electronic and structural properties that surpass those of conventional semiconductors and metals. Furthermore, graphene is also quite unusual electronically since its electric carriers behave as if they were massless and relativistic, the so-called Dirac particles [6, 7]. Graphene research is one of the fastest growing areas in science, but it is still a young field. For these and many other reasons, the graphene field has been surrounded by a lot of hype but also hope. Hope that this material is unveiling the dawn of a new era where carbon, the element of life, also becomes an element of progress.

Therefore, it is of both scientific curiosity and technical importance to understand how these atomically thin sheets assemble, how assembly tailors microstructures, and how microstructures impact on the final material properties.

In our previous work it was shown that the matrix durability properties were improved when carbon nanoma-

terials (CNMs) were incorporated into an electroplated copper matrix [8]. They have a hardening effect on the metal matrix and its hardness increases from $190 \text{ kgf} \cdot \text{mm}^{-2}$ for a pure copper coating to $340 \text{ kgf} \cdot \text{mm}^{-2}$ – for composites. Their electrical properties do not change and have the same coefficient of electric resistivity. The graphene /or graphene oxides incorporated into the copper matrix promoted formation of copper nanocomposites of a new generation.

The present article mainly concerns the morphology and topography of copper composites, namely reinforced with carbon nanomaterials and its influence on wear and corrosion properties of copper coatings. A characteristic feature of most materials is that after long-term usage under unfavourable conditions one or more of their functional properties can degrade [9]. Therefore, the aim of this paper was to study the resistance of the metal-matrix composites Cu-CNMs to both electrochemical corrosion and wear and compare the results obtained with those for pure copper coatings.

EXPERIMENTAL DETAILS

Electroplated $10 \mu\text{m}$ thick copper and copper composite coatings were studied. Copper coatings modified with carbon nanomaterials (CNMs) were electrodeposited in electrolytes containing (mol dm^{-3}): $\text{CuSO}_4 \cdot 5 \text{ H}_2\text{O} - 0.25$, $\text{H}_2\text{SO}_4 - 0.5$ at a cathodic current density (i_c) of $2 \text{ A} \cdot \text{dm}^{-2}$ at $18^\circ\text{C} \pm 1^\circ\text{C}$ and pH 0.8. The agitation conditions of electrolyte were suited to a turbulent fluid flow. The motive force of turbulent fluid flow directed the particles of CNMs to the cathode surface and prevented them from sedimentation in the bulk of electrolyte. The intensity of compressed air was estimated by using a rotameter and was maintained as high as

*Corresponding author. Tel.: +370-5-2649774; fax: +370-5-2648890. E-mail address: viktorija.medeliene@gmail.com (V. Medeliene)

$300 \text{ dm}^{-3} \text{ h}^{-1}$. Electrolytic copper (AnalaR, BDH Chemicals LTD, UK) was used as an anode. Analytical grade chemicals and bidistilled water were used to prepare electrolytes.

The concentration (c) of CNMs in the electrolyte suspension was 0.4 g dm^{-3} . CNMs powder with average size of particles (50–100) nm was used for suspension preparation. The carbon nanomaterials (CNMs) were synthesized at $800^\circ\text{C} \pm 10^\circ\text{C}$ by catalytic chemical precipitation and decomposition of the CH_4 gas by Boudouard reaction using a $\text{Fe}(\text{CO})_5$ catalyst precursor – (CNM1); 5 % H_2S gas was injected into a separate stream of gaseous media – (CNM2); 5 % NH_3 gas was injected into a separate stream of gaseous media – (CNM3).

The surface topography of the coatings was examined in a nanometric scale using Atomic Force Microscopy (AFM). AFM images were recorded in the semi-contact (tapping) mode with a gold-coated Si_3N_4 tip to reveal the topography of the coatings by an Explorer (VEECO Dimension 3100 Microscope), using a Hybrid XYZ scanner with a scan rate of 0.5 Hz/line. All scans were acquired at room temperature under atmospheric pressure and characterized by measuring the arithmetic average of the absolute values of the surface nanoroughness (R_a /or R_{av}) as well as 3D images of phase topography.

The microstructure and elemental composition of Cu and copper nanocomposite coatings were studied and recorded by a scanning electron microscope EVO 50 EP (Carl Zeiss SMT AG, Germany) with an INCA energy dispersive X-ray spectrometer (Oxford Instruments) at an acceleration voltage of 20 kV and an electron beam current (ec) of 150 pA–240 pA.

The surface stability properties after wear and corrosion resistance tests of coatings were determined by dry friction and electrochemical tests. Electrochemical voltammetric (I/E) as well as impedance measurements (Z) were carried out in a naturally aerated acidic (0.5 M $\text{CuSO}_4 \cdot 5 \text{H}_2\text{O} + 0.25 \text{ M H}_2\text{SO}_4$, $\text{pH} = 0.8$) solution. The experiments were conducted at room temperature ($18^\circ\text{C} \pm 1^\circ\text{C}$). A three-electrode cell connected with a computer controlled potentiostat in an AP/G/FRA Autolab 302 apparatus (The Netherlands) was used. In the three electrode system of potentiodynamic polarization measurements at a scan rate of 1 mV s^{-1} , the specimen of investigated nanocomposite copper coatings served as a working electrode with a platinum wire as a counter electrode and Ag/AgCl – as reference. Corrosion current densities (j_{corr}) after 6 hour exposure of coatings in acidic medium were determined by extrapolation of anode and cathode Tafel plots to the potential value E_{ocp} (or E_{corr}). EIS measurements were performed at the E_{corr} (or E_{ocp}) with a perturbation amplitude of 5 mV and in a low frequency range from 100 KHz to 5 mHz. The impedance modulus at a low frequency end of the spectrum ($Z_{f \rightarrow 0}$) was usually interpreted as the complex polarization resistance (R_p). In this work R_p values corresponded to $Z_{f \rightarrow 0.005 \text{ Hz}}$. R_p measurements were started after exposure to corrosive media for 0.5; 1; 2; 4 and 6 hours. All measured spectra were plotted as Bode and Nyquist diagrams.

The wear resistance tests of 6 μm and 20 μm thick copper and copper nanocomposite coatings were

performed at room temperature with a relative humidity of 45 %–55 % under dry friction conditions by sliding of the steel ball under loads of 40 g and 80 g (0.04 N or 0.08 N) on the flat surface of copper coatings. A steel ball of \varnothing of 8 mm ($\text{HV} = 800 \text{ kgf}\cdot\text{mm}^{-2}$) was used as a counterbody (15X steel (GOST 9543-71, Russia). The motion of the ball was linear and reciprocated. Linear wear of specimens was measured by a profilometer-profilograph type 252 (Russia). The total sliding distance was 26 m with overall 1000 sliding cycles. The images of worn specimens or a width of wear scar on the surface were investigated using a MTj Metallurgical Microscope with a 3 Mega Pixel digital camera. A length of the stroke of the worn surface of investigated coatings was $1.3 \text{ cm} \pm 0.1 \text{ cm}$ in the case of brass substrate and $2 \text{ cm} \pm 0.1 \text{ cm}$ – in the case of steel with the nickel overlayer substrate. The damage of metal was expressed as a depth of wear scar (\bar{d}). 20 μm thick copper and copper nanocomposite coatings were electrodeposited on the steel substrate with a 6 μm nickel underlayer which was harder than copper coatings. The profilogrammes of the coating surface were drawn and the micro roughness parameters (R_a) of the surface profile were measured. The measured characteristics R_a are the average values of the arithmetic mean deviation of the middle line of profilogramm. The average value was calculated from 10 measurements.

RESULTS AND DISCUSSIONS

According to the data presented in [8], carbon nanomaterials have no influence on the values of interplanar distances (d) of copper, but it affects the growth of crystallites during electro crystallization and change the type of morphology (Fig. 1). Morphological studies of copper composite coatings formed with carbon nanoderivatives have shown that the copper matrix is composed of larger copper crystallites as compared to of crystallites of copper composite matrixes (Fig. 1). The matrix of composites Cu-CNM3 has a “cauliflower” structure, which is a specific feature of nanocrystalline /or crystallitic coatings. (Fig. 1, d) [10].

As copper is not an inherently reactive element, it is not surprising that the rate of corrosion is usually low. The superior performance of copper is associated with several factors. The main one is that it forms a cuprous oxide (Cu_2O) corrosion product film that is responsible for its protection and is tenaciously adherent [11]. Consequently, corrosive properties of copper and copper composite coatings with nano inclusions of graphene or/ graphene oxide were studied in an aggressive (with respect to metallic copper) acidic (0.25 M $\text{CuSO}_4 \cdot 5\text{H}_2\text{O} + 0.5 \text{ M H}_2\text{SO}_4$) media. It has been established that under the conditions of natural convection and natural aeration, the electrochemical corrosion rate of copper and copper composite coatings (j_{corr}) after six hours of exposure to the acidic medium is $(1.7 \times 10^{-3} \div 2.1 \times 10^{-3}) \text{ A}\cdot\text{cm}^{-2}$ for all copper coatings studied: $1.7 \times 10^{-3} \text{ A}\cdot\text{cm}^{-2}$ for both Cu and Cu-CNM1, $1.9 \times 10^{-3} \text{ A}\cdot\text{cm}^{-2}$ – for Cu-CNM2 and $2.1 \times 10^{-3} \text{ A}\cdot\text{cm}^{-2}$ – for Cu-CNM3 composite coatings (Fig. 2). In the acidic medium a stronger oxidation of copper composites occurred (Fig. 2, b). However, with longer immersion

periods, more corrosion products are formed, resulting in an increase in the polarization resistance (R_p) of corrosion that is more pronounced due to the action of copper corrosion products (CuOH)_{ads}, CuSO_4 _{ads} and CuHSO_4 _{ads} [11]. Eventually, corrosion products cover the whole surface of the specimen and the corrosion rate tends towards a steady value.

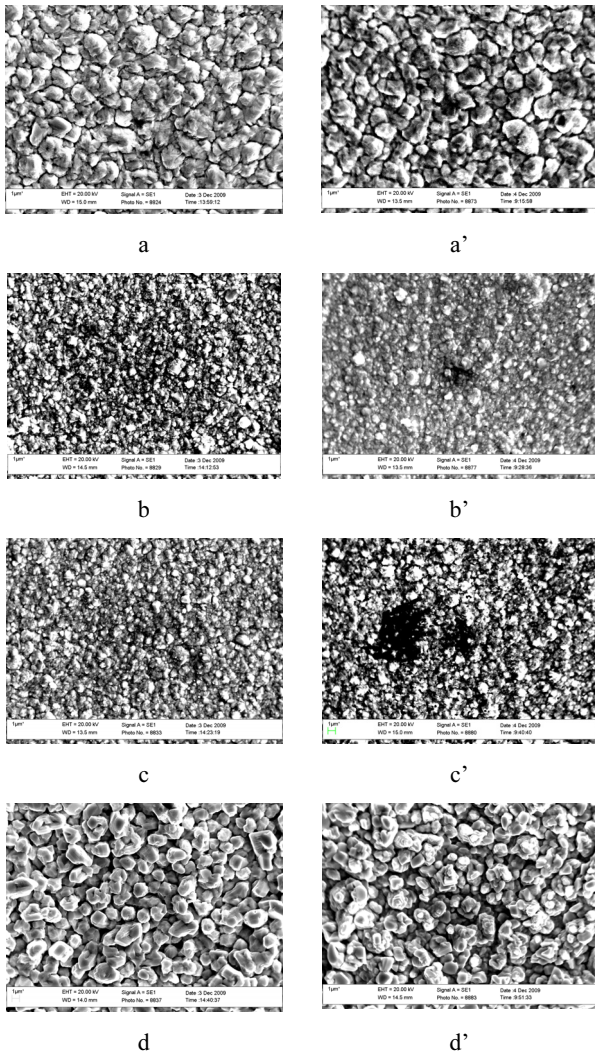


Fig. 1. The microstructure images of copper (a, a') and copper composite coatings Cu-CNM1 (b, b'), Cu-CNM2 (c, c') and Cu-CNM3 (d, d') before (a–d) and after corrosion tests (a'–d'). Concentration of CNMs in electrolyte-suspension – 0.4 g dm⁻³. Magnitude: a, a'–d, d' – ×20000

There is a high probability that a protective film will be formed during immersion periods. The impedance spectra modulus of experimental data presented in the Bode and Nyquist diagrams obtained after 0.5; 1; 2; 4 and 6 hours of continuous exposure to the solution, evidence that the values of surface polarization resistance (R_p) increase with an increase in exposure time owing to the surface interlock with a protective film of insoluble corrosion products: from 24.7 Ω cm⁻² to 25.2 Ω cm⁻² – for Cu, from 14.5 Ω cm⁻² to 23.9 Ω cm⁻² – for Cu-CNM1, from 15.1 Ω cm⁻² to 35.1 Ω cm⁻² – for Cu-CNM2 and from 15.9 Ω cm⁻² to 35.4 Ω cm⁻² for Cu-CNM3 composite coatings (Figs. 3 and 4). The data of microanalysis have

shown that after coatings exposure to the acidic medium for 6 hours a higher oxygen quantity was detected as compared to that of coatings not exposed to the corrosive medium (Table 1).

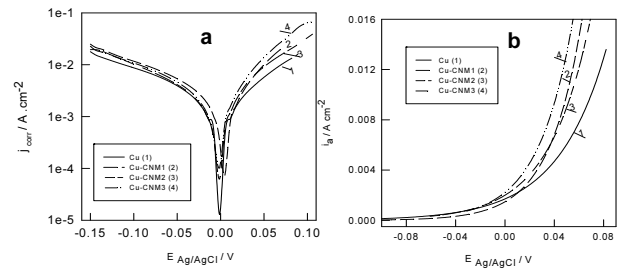


Fig. 2. Voltammetric dependencies – E – $\log j_{\text{corr}}$ (a) and E – i_a (b) obtained after 6 hours exposure in acidic medium at a free corrosion conditions of copper and copper composite coatings: 1 – Cu, 2 – Cu-CNM1, 3 – Cu-CNM2, 4 – Cu-CNM3. E_{ocp} value for Cu coating is 0.007 V, for Cu-CNM1 coating is 0.012 V and for both Cu-CNM2 and Cu-CNM3 coatings are 0.006 V

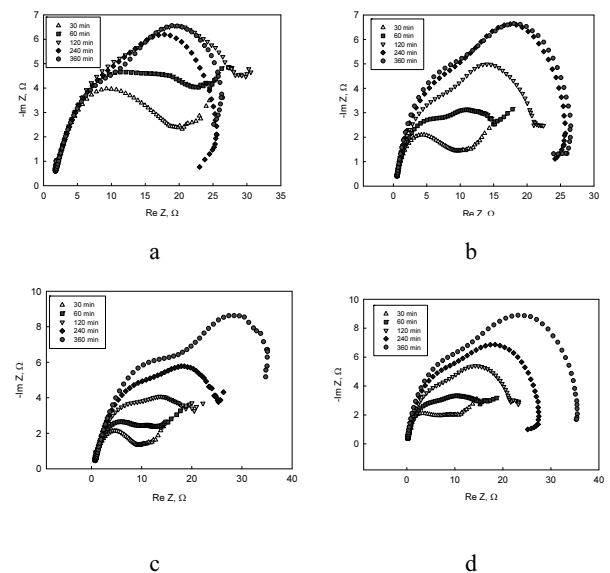


Fig. 3. Nyquist diagrams at the E_{ocp} in the frequency range of 100 KHz $\geq f \geq$ 10 mHz for copper (a) and copper composite Cu-CNM1 (b), Cu-CNM2 (c), Cu-CNM3 (d) coatings vs immersion time from 0.5 to 6 hours in an acidic copper solution at a free corrosion conditions

Table 1. Microanalysis data of oxygen content (at. %) in coatings before and after 6 hours exposure in the acidic medium

Coatings	Before exposure	After exposure
1. Cu	2.1	6.2
2. Cu-CNM1	1.5	7.5
3. Cu-CNM2	2.5	2.6
4. Cu-CNM3	1.6	3.7

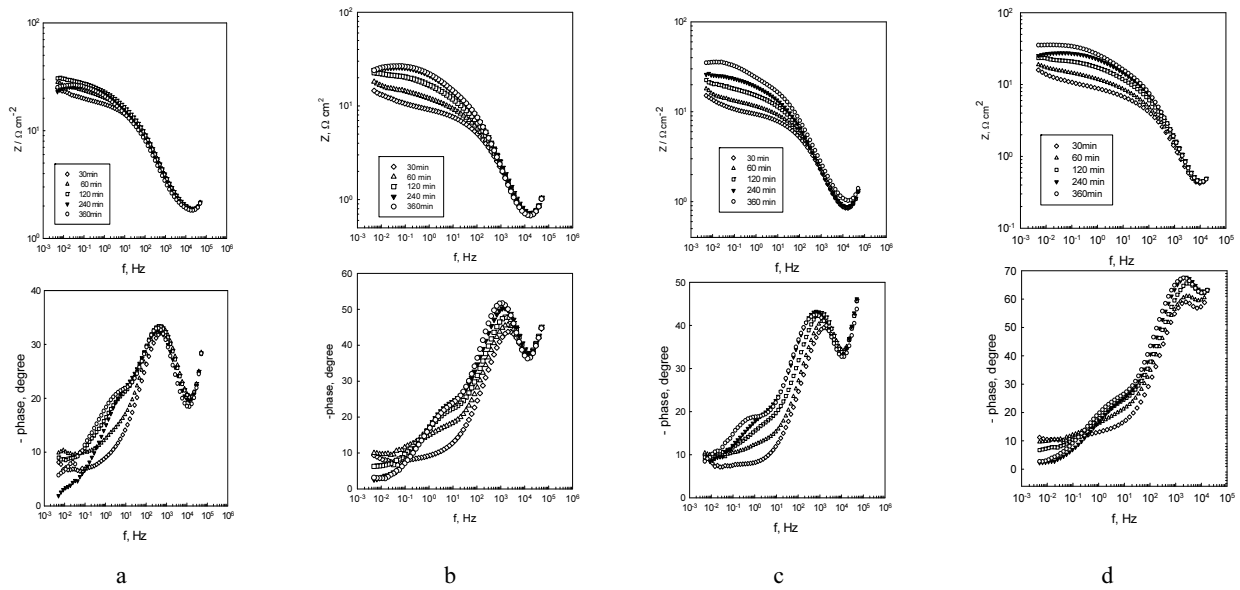


Fig. 4. Bode diagrams of impedance spectra of copper (a) and copper composite Cu-CNM1 (b), CNM2 (c) and CNM3 (d) coatings in the acidic copper solution vs exposure time

Graphite as a well-known material with lamellar structure is widely used as solid additive to form self-lubricating wear resistance coatings [12–16]. The tribological properties of investigated nanocomposite materials with incorporated into matrixes of Cu-CNMs lammellae of graphene /or graphene oxides need to be thoroughly investigated. AFM topography study of coatings has shown that the surface layers of copper nanocomposite coatings are smoother and possess lower values of both surface irregularities (\bar{R}_{max}) and nanoroughness (\bar{R}_a , \bar{R}_{MS}) (Table 2, Fig. 5). The nanoroughness values (\bar{R}_a , \bar{R}_{MS}) obtained for a $2 \mu\text{m}^2$ area of upper surface layer are 2 to 2.5 times lower as compared to those of pure copper. (\bar{R}_a) of pure copper coating reaches 84 nm, while (\bar{R}_a) of copper composite coating is (33 ÷ 43) nm (Table 2). It is evident that lammellae of graphene /or graphene oxides are smoothing additives.

The presence of carbon nanoderivatives CNMs in the copper composite coatings increases their wear resistance (Table 3). Nanocomposites Cu-CNMs possess a higher wear resistance as compared to that of pure copper. In consequence, lammellae of graphene /or graphene oxides incorporated into matrixes of Cu-CNMs coatings act not only as smoothing, but and lubricating additives [8].

The existence of lammellae as a lubricating nanophase is the essential factor that affects the wear resistance of nanocomposites.

It should be mentioned, that the wear mode was based on the metal deformation in the place of friction contact of hard steel counterbody with pure copper and copper composite coatings electrodeposited on the brass substrate. Metal damage expressed as the depth of metal wear (\bar{d}) for copper nanocomposite coatings is less as compared to that of pure copper coating: for Cu-CNM2 is 0.5 μm , for Cu-CNM1 and Cu-CNM3 composites – 1.0 μm and for pure Cu coating is 1.5 μm (Table 3). As a result of the CNMs incorporation into the metal matrix, they can bear a higher contact load. In addition, after six hours of exposure to the acidic corrosive medium the surface wear (\bar{d}) moderately increases, probably owing to easier removal of corrosion products during the wear test (Table 3).

The destruction of surface occurs when another mode of wear is realized with a hard steel slider as a counterbody shearing at the coated contact with a softer coating electrodeposited on the hard substrate of steel and nickel overlayer. In this case wear tracks on the copper composite coatings are broader than those on pure copper (Fig. 6). Copper and copper composite coatings electrodeposited on

Table 2. AFM measurements data of the average values (with bias $\pm\sigma$) of characteristic: surface distribution (\bar{S}); maximum height of surface irregularity (\bar{R}_{max}); geometrical roughness (\bar{R}_{MS}); average (arithmetical) roughness (\bar{R}_a) of overlayer of copper and copper composite coatings with CNMs inclusions electrodeposited on the brass substrate

Coatings	\bar{S} , μm ;	\bar{R}_{max} , nm	\bar{R}_{MS} , nm	\bar{R}_a , nm
1. Pure Cu	1.1 ± 0.5	225 ± 99.5	70.6 ± 31.4	84.0 ± 21.6
2. Cu-CNM1	0.6 ± 0.1	99.9 ± 43.0	27.1 ± 8.9	33.2 ± 12.2
3. Cu-CNM2	0.5 ± 0.01	130.4 ± 48.1	39.4 ± 13.3	36.3 ± 6.9
4. Cu-CNM3	1.0 ± 0.7	96.6 ± 8.1	35.9 ± 13.7	42.9 ± 18.4

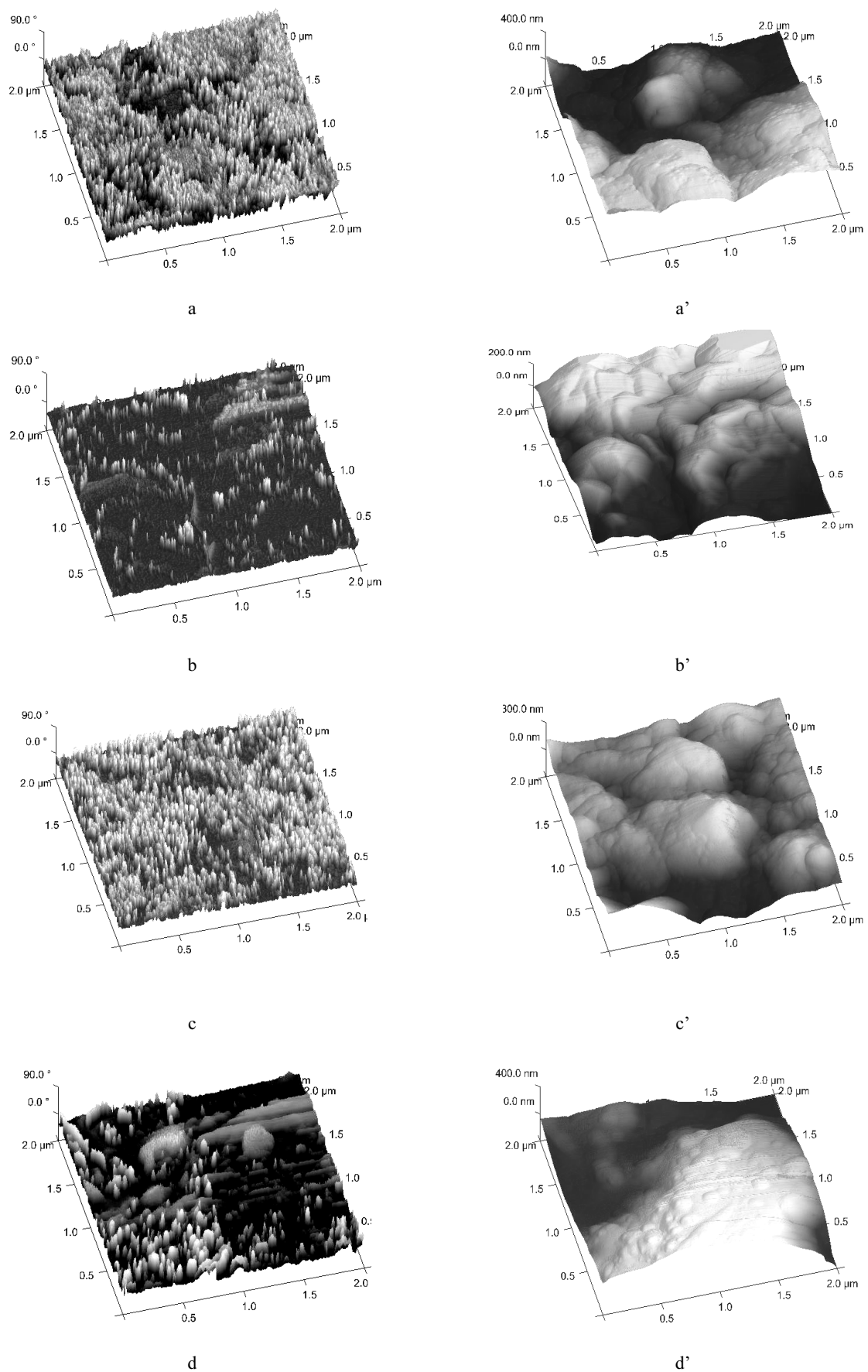


Fig. 5. AFM measurements data of 3D images of phase topography (a–d) and relief (a'–d') of scanned a 2 μm size surface area of overlayer of nanostructured copper and copper composite coatings electrodeposited on the brass substrate. Coatings: a, a'– pure Cu; b, b' – Cu-CNM1; c, c' – Cu-CNM2; d, d' – Cu-CNM3

steel with a nickel underlayer have higher parameters of microroughness values (R_a): Cu-CNM3 = 2.07 ± 0.74 ; Cu-CNM1 = 1.26 ± 0.27 ; Cu-CNM2 = 1.03 ± 0.14 , as compared to those of copper coating (pure Cu = $0.95 \pm 0.20 \mu\text{m}$) (Fig. 7). In this case abrasive wear emerges. The nanoroughness of coating surface changes and microsystems regularities are characteristic of Cu-CNMs coatings. So that the positive properties of nanosurfaces will be preserved, the coatings should be formed on a smooth substrate (Fig. 5).

Wear is generally affected by several factors, among them materials selection, friction, surface load, sliding distance, surface hardness, surface finishing, lubrication,

Table 3. The values of average depth of wear scar (\bar{d} , μm) of copper and copper composite coatings during dry friction under 40 kgf load and after 6 hour exposure in the acidic corrosion medium

Coatings	(\bar{d}) , μm	(\bar{d}) after corrosion test, μm
1. Cu	1.5	1.5
2. Cu-CNM1	1.0	1.0
3. Cu-CNM2	0.5	1.0
4. Cu-CNM3	1.0	1.4

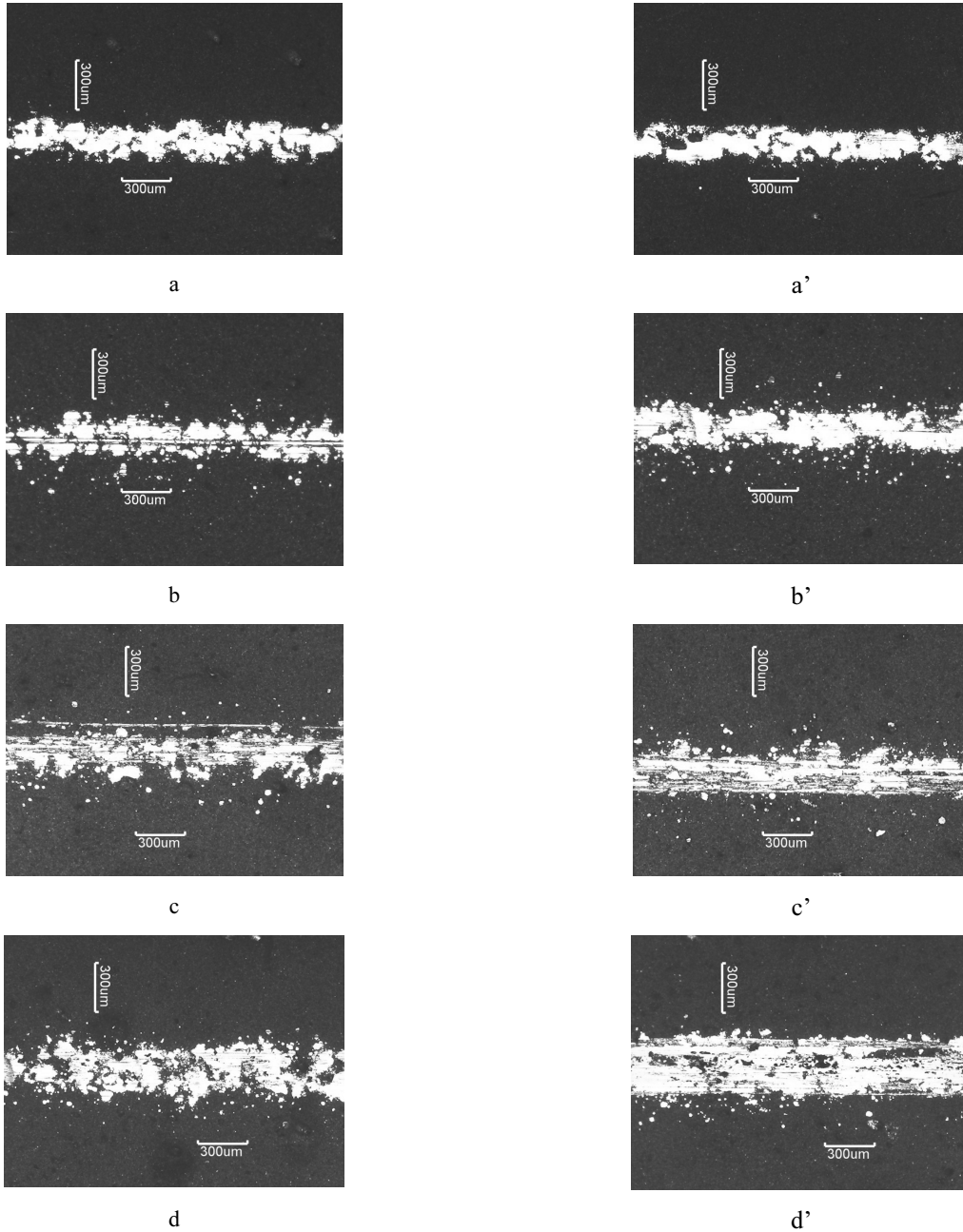


Fig. 6. MTJ images of wear track on copper (a–a') and copper composite coatings with carbon nanomaterials: Cu-CNM1 (b–b'), Cu-CNM2 (c–c') and Cu-CNM3 (d–d'). The applied forces: 40 kgf (a–d) and 80 kgf (a'–d'). Substrate – steel/nickel (6 μm)/copper coatings (20 μm)

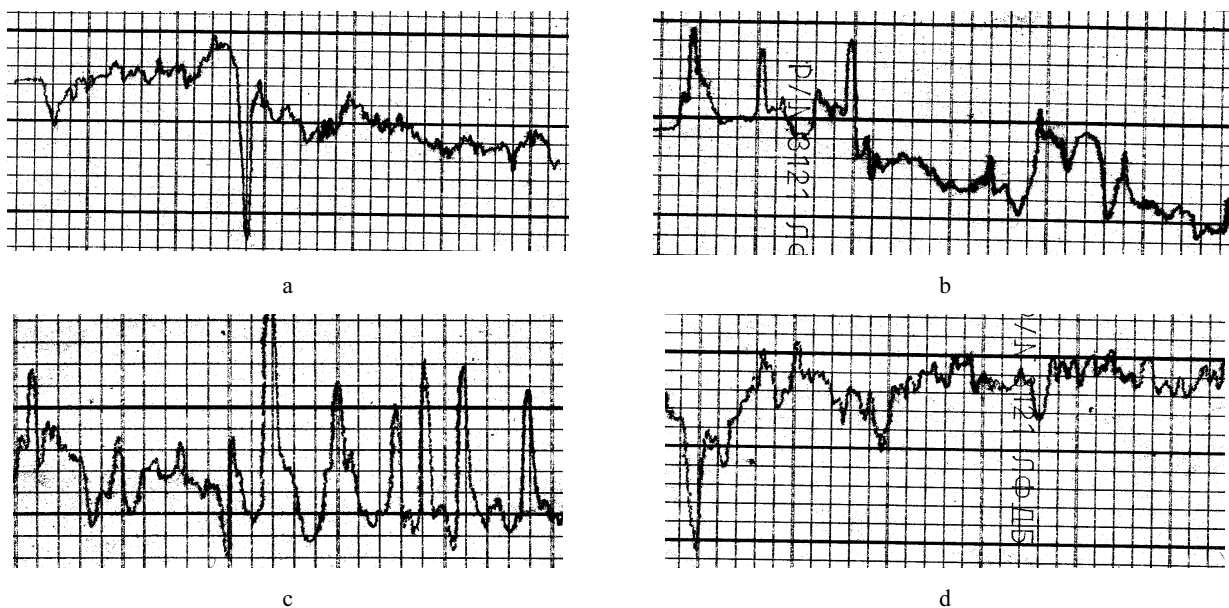


Fig. 7. The profilogrammes of Cu and Cu-CNMs coatings with inclusions of carbon nanomaterials recorded on copper and copper composite coatings of 20 μm thickness electrodeposited on the steel substrate with a 6 μm nickel over layer. a – electrolytic copper without CNM; b – Cu-CNM1; c – Cu-CNM2) and d – Cu-CNM3. The horizontal scale (1 square) of profilogramme for copper and all Cu-CNMs coatings is 40 μm and vertical scales (1 square) are: for Cu; Cu-CNM1; Cu-CNM2, 1 μm ; for Cu-CNM3, 2 μm

etc. Thus, controlling these factors can contribute to a successful application by helping to prevent wear and premature product failure. It is known that wear can be defined as both material loss and/or deformation at contact surfaces. Besides, the heat generated due to the wear is also an important factor affecting the behaviour of wear resistance of materials. Although copper possesses a high thermal conductivity and has a capability to quickly carry away the heat generated by wear process, it is believed that the wear heat induces some oxidation on the tribosurfaces. It should be emphasized that the wear and corrosion properties are complicated due to the environment and wear synergistic effect, which is often encountered in real working situation.

CONCLUSIONS

1. In the acidic medium a stronger oxidation of copper composite coatings with incorporated CNMs occurred. The corrosion rate (j_{corr}) of copper and copper composite coatings after six hours of exposure to the acidic medium is $(1.7 \times 10^{-3} \div 2.1 \times 10^{-3}) \text{A} \cdot \text{cm}^{-2}$ for all copper coatings studied: $1.7 \times 10^{-3} \text{A} \cdot \text{cm}^{-2}$ for both Cu and Cu-CNM1, $1.9 \times 10^{-3} \text{A} \cdot \text{cm}^{-2}$ – for Cu-CNM2 and $2.1 \times 10^{-3} \text{A} \cdot \text{cm}^{-2}$ – for Cu-CNM3 composite coatings. However, with a longer immersion period, more insoluble corrosion products are formed, which leads to an increase in the polarization resistance (R_p) and corrosion protection of composite coatings.
2. Nanocomposites possess a higher wear resistance as compared to that of pure copper and the damage of metal characterized as a depth scar (\bar{d}) is lower. Therefore, the wear resistance of nanocomposites is impaired when they are deposited on a hard steel substrate when abrasive wear emerges. The nanoroughness of coating surface changes to

microroughness. In order to preserve the positive properties of nanosurfaces, the coatings should be formed on a smooth substrate.

REFERENCES

1. **Brodie, B. C.** On the Atomic Weight of Graphite *Philosophical Transactions of the Royal Society of London* 1490 1859: pp. 249–259.
2. **Kim, J., Cote, L. J., Kim, F., Yuan, W., Shull, K. R., Huang, J.** Graphene Oxide Sheets at Interfaces *Journal of the American Chemical Society* 132 (23) 2010: pp. 8180–8186.
3. **Novoselov, K. S., Geim, A. K., Morozov, S. V., Jiang, D., Zhang, Y., Dubonos, S. V., Grigorieva, I. V., Firsov, A. A.** Electric Field Effect in Atomically Thin Carbon Films *Science* 306 (5696) 22 October 2004: pp. 666–669.
4. **Stankovich, S., Dikin, D. A., Dommett, G. H. B., Kohlhaas, K. M., Zimney, E. J., Stach, E. A., Piner, R. D., Nguyen, S. B. T., Ruoff, R. S.** Graphene-based Composite Materials *Nature* 442 20 July 2006: pp. 282–286.
5. **Tian, L., Meziani, M. J., Lu, F., Kong, Ch. Y., Cao, L., Thorne, T. J., Sun, Y.-P.** Graphene Oxides for Homogeneous Dispersion of Carbon Nanotubes *ACS Applied Materials & Interfaces* 2 (11) 2010: pp. 3217–3222.
6. **Horing, N. J. M.** Aspects of the Theory of Graphene *Philosophical Transactions of the Royal Society of London A* 13 December 2010: pp. 5525–5556.
7. **Novoselov, K. S., Geim, A. K., Morozov, S. V., Jiang, D., Katsnelson, M. I., Grigorieva, I. V., Dubonos, S. V., Firsov, A. A.** Two-dimensional Gas of Massless Dirac Fermions in Graphene *Nature* 438 2005: pp. 197–200.
8. **Medelienė, V., Juškėnas, R., Kurtinaitienė, M., Selskienė, A., Stankevič, V.** The Impact of Carbon Nanomaterials on

- the Formation and Properties of Electrodeposited Copper Composite Coatings *Materials Science (Medžiagotyra)* 16 (1) 2010: pp. 35–39.
9. **Lekka, M., Koumoulis, D. N., Kouloumbi, N., Bonora, P. L.** Mechanical and Anticorrosive Properties of Copper Matrix Micro- and Nano- Composite Coatings *Electrochimica Acta* 54 2009: pp. 2540–2546.
 10. **Facchini, D., McCrea, J. L., Gonzales, F., Palumbo, G., Tomantschger, K., Erb, U.** Nanostructured Metals and Alloys – Use of nanostructured Cobalt Phosphorus as a Hard Chrome Alternative for Functional Applications *Jahrbuch Oberflächentechnik* (ISBN 978-3-874880-245-1) 64 2008: pp. 34–45.
 11. **Ogbuji, L.** A Table-Top Technique for Assessing the Blanching Resistance of Cu Alloys *Oxidation of Metals* 63 (5/6) June 2005: pp. 394–399.
 12. **Jones, J. R.** Lubrication, Friction, and Wear. NASA-SP-8063. 1971: 75 p.
 13. **He, D. H., Manory, R.** A novel Electrical Contact Material with Improved Self-lubrication for Railway Current Collectors *Wear* 249 2001: pp. 626–636.
 14. **Donnet, C., Erdemir, A.** Historical Developments and New Trends in Tribological and Solid Lubricant Coatings *Surface and Coatings Technology* 76 2004: pp. 180–181.
 15. **Lee, Ch., Li, Q., Kalb, W., Liu, X-Z., Berger, H., Carpick, R. W., Hone, J.** Frictional Characteristics of Atomically Thin Sheets *Science* 328 2 April 2010: pp. 76–80.
 16. **Medelienė, V.** The Wear Resistance Ability of Copper Metal Matrix Composite Coatings with Microparticles of B₄C and SiC *Jahrbuch Oberflächentechnik* (ISBN 978-3-874880-245-1) 64 2008: pp. 310–318.

Presented at the National Conference "Materials Engineering'2010" (Kaunas, Lithuania, November 20, 2010)